Cronfa - Swansea University Open Access Repository

_____

This is an author produced version of a paper published in:
Solar Energy

_____

Cronfa URL for this paper:

http://cronfa.swan.ac.uk/Record/cronfa40653

_____

Paper:

Stoichkov, V., Bristow, N., Troughton, J., De Rossi, F., Watson, T. & Kettle, J. (2018). Outdoor performance monitoring of perovskite solar cell mini-modules: Diurnal performance, observance of reversible degradation and variation with climatic performance. _Solar Energy, 170_, 549-556.

http://dx.doi.org/10.1016/j.solener.2018.05.086

_____

http://www.swansea.ac.uk/library/researchsupport/ris-support/

Outdoor performance monitoring of perovskite solar cell mini-modules: diurnal performance, observance of reversible degradation and variation with climatic performance

V. Stoichkov[1], N Bristow[1], J. Troughton[2], F. De Rossi[2], T.M. Watson[2], J. Kettle[1]

[1]*School of Electronic Engineering, Bangor University, Dean St, Gwynedd, Bangor, LL57 1UT, Wales, UK. *E-mail: j.kettle@bangor.ac.uk*

[2]*SPECIFIC, Swansea University Bay Campus, Fabian Way, Swansea SA1 8EN, United Kingdom*

Abstract

The outdoor performance monitoring of two types of perovskite solar cell (PSC) mini-modules based on two different absorbers - $CH_3NH_3PbI_3$ (MAPI) and $Cs_{0.05}FA_{0.83}MA_{0.17}PbI(_{0.87}Br_{0.13})_3$ (FMC) is reported. PSC modules displayed markedly different outdoor performance characteristics to other PV technologies owing to the reversible diurnal changes in efficiency, difference in temperature coefficient between absorber layers and response under low light conditions. Examination of diurnal performance parameters on a sunny day showed that whereas the FMC modules maintained their efficiency throughout the day, the MAPI modules peaked in performance during the morning and afternoon, with a strong decrease around midday. Overall, the MAPI modules showed a strongly negative temperature coefficient (TC) for PCE, whereas the FMC modules showed a moderate positive temperature coefficient performance as a function of temperature due to the increase in J_{SC} and FF. Outdoor monitoring of the MAPI modules over several days highlighted that the reduced over the course of the day but recovered overnight. In contrast the FMC modules improved slightly during the daytime although this was too reversed overnight. This paper provides insight into how PSC modules perform under real-life conditions and consider some of the unique characteristics that are observed in this solar cell technology.

Keywords; outdoor monitoring, perovskite solar cell, PSC temperature coefficient

1. Introduction

Research into Perovskite Solar Cells (PSCs) has grown exponentially over the last decade as PSCs provide the potential for low cost and solution-based production, on flexible substrates, and at lower temperatures than silicon cells, thus reducing the embodied energy. At present PSCs only moderately lag silicon based solar cells in terms of power conversion efficiency (PCE), with the best reported cells possessing a PCE of 22.7% and mini-modules reported up to 16% [1], [2].

In order for these emerging PV technologies to become commercially viable it is important that it is understood how they perform under real world conditions. Such testing is crucial for understanding how performance is affected by climatic changes such as irradiance level and allows technologists to evaluate the challenges in integrating the technology with existing energy and building infrastructure. Furthermore, it provides valuable information on stability; in the outdoors, the solar cell experience multiple stresses, rather than just one, that continuously vary with time including light, temperature, condensation, wind as well as humidity, temperature and light cycling. Numerous studies have addressed instability of perovskite and transport- layers in PSCs induced by heat [3], UV light [4], [5], electric field and humidity [6] and in real outdoor operational conditions many of these factors simultaneously act upon the PSC. However, there are relatively few reports of outdoor performance monitoring of PSCs. This is for a number of reasons including amongst others the problems of scalability, such as the higher sheet resistivity of transparent conducting oxides leads to drops in PCE [7] , as devices get larger. Specialised equipment is needed for the characterisation of large area modules that is not readily available in most PV laboratories. Furthermore, small devices are difficult to measure outdoors with high accuracy, as the currents involved are small (nA), especially at lower irradiances, and require the use of specialist test equipment, which has impeded studies on outdoor testing [8], [9].

Misra et al. [10], [11] were one of the first groups to use sunlight and study the degradation giving invaluable insight to the community towards the stability of the PSC to light-induced degradation. In 2015 Li et al. [12] demonstrated the first results from PSCs exposed outdoors with no UV filtration in Saudi Arabia following the ISOS O1 protocol and showed stable performance for up to 7 days with no drop in performance. In 2016 Reyna et al. [13] presented their work on mixed halide PSCs mounted on a solar tracker with over 1000 hours outdoor exposure, showing that $T_{80\%}$ occurred at 846 hours and also demonstrated the enhanced stability of $FAPbI_3(0.85)MAPbBr_3(0.15)$ over conventional $MAPbI_3$ perovskite devices. Nevertheless, even this composition for PSCs was found to be highly susceptible to UV light and quality of edge-sealant, which were deemed to be the main causes for degradation.

In this work, a comparison of performance parameters as a function of irradiance and temperature for Single cation, single halide $MAPbI_3$ (MAPI) and triple cation, mixed halide (FMC) perovskite mini-modules are reported. Furthermore, the dependence of module temperature rise above ambient as a function of irradiance is analysed for both PSC modules and compared to c-Si modules, leading to calculated values for the Ross coefficient. The effect of wind speed on the Ross coefficient is also examined. Also, the reversibility of certain PSC degradation processes is reported by comparing PV performance on consecutive days. Stability studies on PSC modules are also

presented showing that long-term stability is achievable, although performance is inhibited by a temporary reversible degradation during the initial burn-in period.

2. Experimental details

2.1 Active layer fabrication details

Mini-modules manufactured with $CH_3NH_3PbI_3$ (MAPI) and $Cs_{0.05}FA_{0.83}MA_{0.17}PbI(_{0.87}Br_{0.13})_3$ (FMC) perovskite mini-modules were used in this work [14]. The final manufactured modules were 5cm x 5cm in size and consist of five serially connected cells with 2.7 cm^2 per cell and 13.5 cm^2 total active area, device geometric fill factor was 0.54.

Both MAPI and FMC were prepared from solution on ITO-coated glass (7Ω/sq). A NiO$_x$ hole transport layer is obtained by spin coating a solution of 0.22M nickel acetate tetrahydrate dissolved in a 1:0.012 vol ratio of 2-methoxyethanol:ethanolamine at 3500 rpm for 30s. The formed layer was annealed at 250°C for 60 min before cooling to room temperature. The MAPI precursor solution was prepared by dissolving 576 mg PbI$_2$ and 199 mg MAI in 0.8 ml DMF and 0.2 ml DMSO. The FMC solution was prepared by dissolving PbI$_2$ (0.35 g), FAI (0.12 g), MAI (0.035 g), CsI (0.026 g) and PbBr$_2$ (0.09 g) in 0.8ml of DMF and 0.2ml DMSO. Both structures were deposited using a one-step method using ethyl acetate as antisolvent. The electron transport layer used in this work was PC$_{60}$BM, spin coated from a 20 mg/ml solution in chlorobenzene at 2000 rpm for 30 s. A bathocuproine (BCP) (0.5 mg/ml in anhydrous ethanol) contact layer was spin-coated at 6000 rpm for 15 s. Finally, 100nm Ag contacts were added by thermal evaporation. For module patterning, the P1 was defined by laser scribing of the substrate ITO, P2 was scribed using a scalpel blade, and P3 was defined by evaporating the electrode metal though a shadow mask. Finally, a light curable epoxy (Ossila) and a thin glass cover were used for encapsulation. Wires were soldered to the Ag contacts and then covered by a UV-curable epoxy (Threebond) which acted as edge sealant.

2.2 Module encapsulation

Six modules were tested for this work and bonded to the centre of a 205mm x 160mm glass backplane and were covered with a commercially available UV filter [14] which filters the UV component of sunlight. Data is presented for the median device. After the UV filter was added, the final stage of the encapsulation was concluded by sealing the edges of the modules with low temperature two part fast curing sealing epoxy supplied by Dyesol UK ltd (now Greatcell Solar ltd.) [15].

For this experiment, all modules were initially tested indoors using a Newport 94021A class ABB standard AM1.5G solar simulator, to ensure that all devices showed consistent performance prior to outdoor testing. The modules were then laminated onto glass substrates and covered with a UV filter before being retested. The average device photovoltaic performance of each type was as follows: MAPI - short-circuit density (J_{SC}) = 2.38 mA/cm^2, open-circuit voltage (V_{OC}) = 5.20V, fill factor (FF) =39.9%, power conversion efficiency (PCE) = 4.92%; FMC - J_{SC} = 2.55mA/cm^2, V_{OC} = 5.40V, FF = 43.0%, PCE = 5.92%.

2.3 Outdoor setup

The outdoor experiments were performed over two campaigns in April and June 2017 at the School of Electronics, Bangor, Gwynedd, North Wales at coordinates latitude 53.228°N, longitude -4.129°W and altitude approximately 20m above sea level. The performance monitoring of the poly-Si module is conducted using a PVMS250 PV measurement system (Egnitec, UK) and the perovskite mini-modules were measured using a Botest SMU. The poly-Si modules are kept at maximum power point in between periodic current-voltage (IV) sweeps (once every minute). Each module has a PT100 temperature sensor fixed to its backplane. Current and voltage at the maximum power point (I_{MPP}, V_{MPP}) and temperature measurements are taken every 15 s. The perovskite mini-modules were kept at open-circuit between IV sweeps conducted once every 15 minutes. All mini-modules also had PT100 sensors constantly reading the module temperature. For these tests, all monitored modules were mounted in-plane towards the sun at an angle of 36° (the optimum for this latitude).

During the outdoor testing, the incident irradiance was monitored using IMT silicon solar reference cells. The weather conditions were constantly recorded using a dedicated weather station setup. The outdoor measurement setup conforms to the ISOS-O2 outdoor measuring protocol [16]. The data were analysed using a combination of MySQL, MS Access, and MS Excel.

3. Results

3.1 Diurnal performance

PSCs were monitored in the period from the 12th June 2017 until the 12th July 2017. Throughout the entire period of this investigation the incident irradiance, weather conditions and module temperature were monitored alongside the IV date from the modules. The measured relative humidity levels were 80% with an average maximum of 90% and average minimum of 61%. The average mean UV index was 1.19 with an average minimum of 1.07 and an average maximum of 5.45. The mean irradiance was 278 W/m^2 with an average maximum of 858 W/m^2, and the average daily insolation over this period was 466 mWh/cm^2.

Initially, an evaluation of the diurnal performance was conducted; therefore, a sunny day was identified during the first week of the measurement campaign (17/06/2017, see Fig. 1) and the performance of the PSC modules was compared against a polycrystalline-silicon (poly-Si) module. Shown in figure 2 are the diurnal performances of both MAPI and FMC against poly-Si showing how the solar cell performance parameters vary over the course of a day. The results show some interesting trends, in particular for the MAPI device.

Interestingly, a small drop in PCE is seen in the poly-Si module from midday onwards due to the negative temperature coefficient of poly-Si, however, this is not observed in the FMC module, indicating that either the temperature coefficient does not impact as much upon PCE or the module temperature does not rise as quickly as a poly-Si module, which is discussed more in the following sections.

In order to evaluate the performance under different light conditions, figure 3 was plotted which shows how the solar cell performance parameters change as a function of in-plane irradiance. It is worth noting that the data shown in figure 3 also shows the indirect temperature dependence; as at higher irradiance, the module temperature is higher (which is discussed later). Whilst the FMC and poly-Si devices possess values of J_{SC} that track the in-plane irradiance closely, the MAPI device shows a poorer response in relationship with higher irradiance over the course of the day. As the V_{OC} and FF are relatively constant during the day for all modules, the PCE is approximately constant from 10 am till 4 pm for the FMC and poly-Si modules, but a drop in PCE is observed in the MAPI module due to the non-proportional value of J_{SC} compared to the irradiance at this point of the day. This is probably resulting from formation of metastable traps inside the active layer over the course of the day [17]. In figure 3(c) the V_{OC} dependence upon irradiance is shown for the MAPI and FMC modules. As to be expected, it demonstrates a logarithmic dependence on irradiance in common with other technologies [18,19]. The FMC module shows a linear dependence of J_{SC} upon irradiance level [19], [20], but the J_{SC} of the MAPI module shows a sub- linear relationship with irradiance, indicating some current limiting at higher irradiances.

The data was separated into morning and afternoon data. Interestingly, there appears to be a discrepancy in the solar cell behaviour depending upon whether the data was collated in the morning or afternoon. For the MAPI modules, it is evident that the solar cell performs better in the morning than it does in the afternoon, which is driven by changes in FF and J_{SC}. The drop in FF and J_{SC} during the day is likely to be due to a combination of reasons. Firstly, it is likely to be related to temperatures, which leads to higher recombination resulting from formation of metastable traps inside the active layer. As demonstrated by Reyna *et al.* [13], all performance parameters suffer a

performance drop with increasing temperature and this is consistent with our findings. This leads to an increase in the series resistance which impedes the movement of carriers within the module leading to a consequential reduction in the generated photocurrent. A second reason could be related to the low FF observed with the MAPI modules (the maximum measured is 34% during this day). As demonstrated by Katz et al for the cells with high value of series resistance (R_s), a sub-linear relationship between J_{SC} and irradiance can be explained by a monotonic increase in the cell's series resistance losses with increase irradiance [22]. This is known to result initially in a decrease of the FF, which is also consistent with our findings in figure 2(d). An increase in R_S is known to result initially in a decrease of the FF, which is consistent with our findings in figure 2(d), and leads to a sub-linear dependence of J_{SC} on the irradiance level. Thirdly, the incident spectrum is changes from higher UV content in the morning to high IR content in the evening, which is likely to lead to a drop in PCE in MAPI cells during the day.

In the case of the FMC module, a reverse behaviour is noted and the module shows enhanced performance in the afternoon and this appears to be driven by changes in FF, and to a lesser extent V_{OC}. This is likely to be due to the filling of traps by the photogenerated carriers as the device is light soaked during the course of the day, as also observed by Shao *et al.* [23].

Recently, there have been many reports of reversibility to PSC degradation processes. A number of papers have considered the partial recovery of solar cell performance under dark conditions [24]–[26]. The root cause of the reversible degradation has not decisively been attributed to a single cause, but is likely to be related to either metastable defect or trap changes which are reversed overnight, or reversible changes in ion redistribution under illumination [23].

In figure 4 morning and evening IV curves are shown for FMC and MAPI modules from two consecutive sunny days. The measurements were taken at similar low irradiance levels (~287 W/m^2) and the current was linearly adjusted to 1000 W/m^2. Table 1 shows the performance parameters obtained from the data. In the case of the MAPI module, the I_{SC} and FF are reduced in the evening; however, this is almost fully recovered by the morning on the subsequent day.

The data in figure 4 shows that in case of MAPI there is a reversible degradation in I_{SC}, recovering fully by the next morning, whereupon the pattern is repeated consistently during the measurement campaign. The loss could be attributed to the accelerated interfacial recombination among the MAPI and the charge selective contacts which have been reported by Zhang et al. [1]. Nie *et al.* [17] accredited the reversible degradation in I_{SC} to the formation of metastable deep traps in the perovskite layer. Nevertheless, there is also an observed loss in V_{OC} of nearly 0.5V which becomes apparent in the evening of the second sunny day which is a clear sign of the initiation of an

irreversible degradation path [24]. Over the course of the two sunny days the FMC module shows a drop in V_{OC} during the day followed by a recovery/increase in the evening time, a result seen by Ogoshi *et al.* [27] and later by Khenkin *et al.* [24] where they attribute the observation to the accumulation of charges at the interface between the active layer and charge transport layers or to increased surface recombination. Domanski and Bag *et al.* [28], [29] attribute the observation to be due to trap formation causing changes in charge extraction or light dependent ion diffusion.

3.2 Effect of temperature on PSC performance

Initially the general trend of module temperature versus solar cell performance have been calculated and plotted in figure 5. To achieve this, data captured at particular irradiance levels during the first week of testing has been filtered so that only one climatic condition is varying within the dataset (temperature). Shown in figure 5 is the temperature dependence of PV performance parameters at a fixed irradiance levels (600 ± 10 W/m^2 and 1000 ± 10 W/m^2). Date was collated during the first week of outdoor monitoring in order to eliminate the effect of module degradation.

The MAPI modules show the greatest temperature dependence, which is more pronounced at the lower irradiance level (600 W/m^2) at -0.105 %/K than the higher irradiance level (1000 W/m^2) at -0.024%/K. At the higher irradiance the performance parameters are almost stable over the range measured and the relatively minor temperature changes has a minimal effect. In the case of FMC module, the temperature dependence is almost negligible within this temperature range. At the higher irradiance level, the modules demonstrate a small drop in V_{OC}, which is overwhelmed by increases in J_{SC} and FF leading to a slight positive PCE coefficient (+0.0078 %/K). This is particularly interested as very few PV technologies possess a positive temperature coefficient in outdoor conditions (OPVs and DSCs are the exceptions) [9] which supports the indoor data supplied by Leong et al. [28].

The Ross coefficient is very often reported in solar cells and shows how the temperature of the module rises as a function of irradiance and varies as a function of material system, absorption of infrared radiation and thermal emissivity of the module. To date there have been no reports of Ross coefficient for PSCs. To calculate the Ross coefficient initially the examination of the rise in module temperature above ambient vs. irradiance is needed (see Figure 6(a)) which shows a linear relationship defined by Eq. (1), where *G* is irradiance and *k* is the slope, known as the Ross coefficient [30].

$$T_{DELTA} = T_{module} - T_{ambient} = kG \qquad (1)$$

The Ross coefficients obtained for the FMC modules (0.0223 K m^2/W) and MAPI modules (0.0234 K m^2/W) at wind speeds below 0.4m/s are very similar, indicating that these modules have similar thermal characteristics. Temperature rise as a result of incident light can occur due to direct absorption from IR, thermalisation losses from other parts of the solar spectrum and absorption by contacts/encapsulants etc. Visoly-Fisher *et al*. showed OPV devices can rise in temperature with exposure to sunlight even with the IR part of the spectrum omitted [30]. The figures for Ross coefficient are slightly lower than those obtained in previous experiments by this group on organic photovoltaic (OPV) modules (0.027 K m^2/W) and polycrystalline (poly-Si) modules (0.028 K m^2/W) [9]. The difference is partly due to the location of the PT100 temperature sensor which was positioned behind the glass substrate that the modules were laminated onto, and partly due to the large substrate to active area ratio; both these factors leading to temperature loss and a reduction in the Ross coefficient. It would be expected that the Perovskite modules would have a similar or higher Ross coefficient than the OPVs as they absorb further into the infrared region (750 nm) than OPVs (650 nm) [31], [32], but could also be due to the increased absorption of other layers (such as the contacts,) or greater thermalisation losses.

Figure 6(b) compares how the Ross coefficient changes with increasing wind speed for Perovskite, OPV and poly-Si modules. All the modules show the Ross coefficient reducing with increasing wind speed, with the rate of reduction dropping towards zero as the wind speed reaches 5-6 m/s. During the period when the Perovskite modules were being tested there were no periods with wind speeds above 4 m/s, but this effect can still be seen and an extrapolated line of best fit is shown. The rate of reduction is related to the differences in thermal mass of the modules in relation to their active area: the OPV module (PET-cell-PET) and the Perovskite module (which has a large area of glass for a small active area) show a large relatively drop in their Ross coefficients; whereas the poly-Si module (glass-cell-tedlar) has a lower drop in Ross coefficient [33], [34]. In the case of MAPI modules, possessing a lower Ross coefficient and be perceived as an advantage, as MAPI modules show a negative temperature coefficient. Despite possessing a negative temperature coefficient, their performance does not drop so severely as the temperature rise under the same irradiance conditions when compared to other technologies such as OPVs or poly-Si.

3.3 Degradation of PSC modules

Finally, modules were studied for degradation; shown in figure 7 is how the performance parameters change as a function of time based upon data obtained at an in-plane irradiance of 600W/m^2. In both cases, despite the glass-on-glass encapsulation and UV filters, all PSC modules,

were seen to degrade within 1 month. Edge sealant was provided from Dyesol UK ltd and the properties of this are well-studied as a stable sealant leading to OPV outdoor performance greater than 1 years in this laboratory.

All performance parameters show relatively constant behaviour over the first 10 days, however, from day 10 the MAPI module starts to degrade, driven initially by changes in J_{SC} and FF. V_{OC} remains relatively resilient and demonstrates only a minor deterioration between weeks one and two, but sees a sudden drop in the third week (which was also observed to the V_{OC} and FF). This was evidently due to the encapsulation failing and substantial water ingress causing complete active layer decomposition [35],[36], [37]. Whilst large amounts of 'liquid water' were not observed inside the cell in week one (as was evident by week four), some evidence of condensation was observed in week two indicating failure of the edge sealant. This is shown in the photos in figure 8; the photographs show how water and oxygen can penetrate through the edges leading to chemical decomposition of all intermediate, active and electrodes layers. It is well known that PSC are shown to be susceptible to oxygen and water-induced degradation [38], [39], so is not surprising that the failure was catastrophic at this point. It is important to note this edge sealant, which is based upon a thermosetting epoxy, has been used before in OPV and dye sensitised solar cell modules, with similar size modules and also on glass substrate and has been shown to achieve over one year of outdoor performance. The fact that the modules failed due to breach encapsulation suggests that alternative edge sealant might be needed for PSCs.

The data does support the view that FMC modules are more stable than MAPI modules and the data verifies that this is true for outdoor conditions and when multiple stresses are exerted onto the modules. The reason behind the superior stability of the FMC modules relates to the improved thermal stability of formamidinium-containing perovskites, and the inclusion of caesium (Cs+) in the complex compound stabilises the photoactive 'black phase' of said perovskite. Deepa *et al.*[40] demonstrate that the optimum quantity of Cs+ is 5% yielded the best efficiency owing to the highest FF, but most significantly that the Cs+ contains the stoichiometric ratios and valance band in perovskite.

Conclusion

This paper examines the outdoor performance of two types of perovskite mini-modules: with $CH_3NH_3PbI_3$ (MAPI) and $Cs_{0.05}FA_{0.83}MA_{0.17}PbI(_{0.87}Br_{0.13})_3$ (FMC). Measurement of diurnal performance parameters on a sunny day showed that whereas the FMC modules maintained their efficiency

throughout the day, the MAPI modules showed peak performance during the morning and afternoon. The MAPI were shown to have a strongly negative temperature coefficient (TC) for PCE, whereas the FMC modules had a slightly negative TC for PCE at lower irradiances and this changed to being slightly positive at higher levels of irradiance. Therefore, it appears that FMC-based PSCs represent one of the few technologies that possess a positive temperature coefficient alongside OPVs and DSCs. Examination of the performance of the modules over several days highlighted that the PCE performance of the MAPI reduced over the course of the day and then recovered overnight, whereas the FMC improved slightly during the daytime although this was reversed overnight. Examination of IV curves from consecutive days showed that I_{SC} and FF for the MAPI displayed reversible degradation each day whereas V_{OC} slowly degraded over time with no obvious reversal. In contrast the FMC modules showed consistent FF and J_{SC} throughout the day, whereas V_{OC} improved during the course of each day and then returned to its original value by the next morning. Examination of the module temperature rise against irradiance allowed the Ross coefficient to be calculated for both module types. Overall these results confirm the improved stability of FMC as compared to MAPI modules outdoors, but both modules degraded rapidly due to breach of the edge sealant.

References

[1]   M. A. Green, Y. Hishikawa, E. D. Dunlop, D. H. Levi, J. Hohl-Ebinger, and A. W. Y. Ho-Baillie, "Solar cell efficiency tables (version 51)," *Prog. Photovoltaics Res. Appl.*, vol. 26, no. 1, pp. 3–12, 2018.

[2]   National Renewable Energy Laboratory (NREL), "Best Research Cell Efficiencies Chart." [Online]. Available: https://www.nrel.gov/pv/assets/images/efficiency-chart.png. [Accessed: 10-Dec-2017].

[3]   G. Niu, X. Guo, and L. Wang, "Review of recent progress in chemical stability of perovskite solar cells," *J. Mater. Chem. A*, vol. 3, pp. 8970–8980, 2015.

[4]   A. A. Melvin, V. D. Stoichkov, J. Kettle, D. Mogilyansky, E. A. Katz, and I. Visoly-Fisher, "Lead iodide as a buffer layer in UV-induced degradation of CH3NH3PbI3films," *Sol. Energy*, vol. 159, no. December, pp. 794–799, 2018.

[5]   H. S. Anizelli *et al.*, "Application of luminescence downshifting materials for enhanced

stability of CH3NH3PbI3(1-x)Cl3xperovskite photovoltaic devices," *Org. Electron. physics, Mater. Appl.*, vol. 49, pp. 129–134, 2017.

[6] D. Bryant *et al.*, "Light and oxygen induced degradation limits the operational stability of methylammonium lead triiodide perovskite solar cells," *Energy Environ. Sci.*, vol. 9, no. 5, pp. 1655–1660, 2016.

[7] M. Jørgensen *et al.*, "The state of organic solar cells - A meta analysis," *Sol. Energy Mater. Sol. Cells*, vol. 119, pp. 84–93, 2013.

[8] N. Bristow and J. Kettle, "Outdoor performance of organic photovoltaics: Diurnal analysis, dependence on temperature, irradiance, and degradation," *J. Renew. Sustain. Energy*, vol. 7, no. 1, 2015.

[9] N. Bristow and J. Kettle, "Outdoor organic photovoltaic module characteristics: Benchmarking against other PV technologies for performance, calculation of Ross coefficient and outdoor stability monitoring," *Sol. Energy Mater. Sol. Cells*, vol. 175, no. October 2017, pp. 52–59, 2018.

[10] R. K. Misra *et al.*, "Temperature- and Component-Dependent Degradation of Perovskite Photovoltaic Materials under Concentrated Sunlight," *J. Phys. Chem. Lett.*, vol. 6, no. 3, pp. 326–330, 2015.

[11] R. K. Misra *et al.*, "Effect of Halide Composition on the Photochemical Stability of Perovskite Photovoltaic Materials," *ChemSusChem*, vol. 9, no. 18, pp. 2572–2577, 2016.

[12] X. Li *et al.*, "Outdoor performance and stability under elevated temperatures and long-term light soaking of triple-layer mesoporous perovskite photovoltaics," *Energy Technol.*, vol. 3, no. 6, 2015.

[13] Y. Reyna, M. Salado, S. Kazim, A. Pérez-Tomas, S. Ahmad, and M. Lira-Cantu, "Performance and stability of mixed FAPbI3(0.85)MAPbBr3(0.15) halide perovskite solar cells under outdoor conditions and the effect of low light irradiation," *Nano Energy*, vol. 30, no. August, pp. 570–579, 2016.

[14] Solaronix, "UV Filter Adhesive Film." [Online]. Available: http://shop.solaronix.com/uv-filter-adhesive-film.html. [Accessed: 10-Jan-2018].

[15] "Dyesol (greatcellsolar)." [Online]. Available: http://www.greatcellsolar.com/about-us/.

[16] M. O. Reese *et al.*, "Consensus stability testing protocols for organic photovoltaic materials and devices," *Sol. Energy Mater. Sol. Cells*, vol. 95, no. 5, pp. 1253–1267, 2011.

[17] W. Nie *et al.*, "Light-activated photocurrent degradation and self-healing in perovskite solar cells," *Nat. Commun.*, vol. 7, 2016.

[18] N. K. Elumalai and A. Uddin, "Open circuit voltage of organic solar cells: an in-depth review," *Energy Environ. Sci.*, vol. 9, no. 2, pp. 391–410, 2016.

[19] G. V. Maria Carmela Di Piazza, "Photovoltaic Sources: Modelling and Emulation."

[20] R. Steim, "The Impact of Interfaces on the Performance of Organic Photovoltaic Cells."

[21] S. Shao *et al.*, "Efficient Perovskite Solar Cells over a Broad Temperature Window: The Role of the Charge Carrier Extraction," *Adv. Energy Mater.*, vol. 7, no. 22, 2017.

[22] M. V. Khenkin, *et al.* "Dynamics of Photoinduced Degradation of Perovskite Photovoltaics: From Reversible to Irreversible Processes." *ACS Applied Energy Materials* vol. 1, No. 2 pp 799-

806, (2018)

[23]   S. W. Lee *et al.*, "UV Degradation and Recovery of Perovskite Solar Cells," *Sci. Rep.*, vol. 6, 2016.

[24]   E. T. Hoke, D. J. Slotcavage, E. R. Dohner, A. R. Bowring, H. I. Karunadasa, and M. D. McGehee, "Reversible photo-induced trap formation in mixed-halide hybrid perovskites for photovoltaics," *Chem. Sci.*, vol. 6, no. 1, pp. 613–617, 2015.

[25]   T. Ogoshi, M. Hashizume, T. Yamagishi, and Y. Nakamoto, "Synthesis, conformational and host–guest properties of water-soluble pillar[5]arene Electronic Supplementary Information (ESI)," *Chem. Commun.*, vol. 4, no. c, pp. 1–5, 2010.

[26]   M. Bag *et al.*, "Kinetics of Ion Transport in Perovskite Active Layers and Its Implications for Active Layer Stability," *J. Am. Chem. Soc.*, vol. 137, no. 40, pp. 13130–13137, 2015.

[27]   K. Domanski *et al.*, "Migration of cations induces reversible performance losses over day/night cycling in perovskite solar cells," *Energy Environ. Sci.*, vol. 10, no. 2, pp. 604–613, 2017.

[28]   W. L. Leong *et al.*, "Identifying Fundamental Limitations in Halide Perovskite Solar Cells," *Adv. Mater.*, vol. 28, no. 12, pp. 2439–2445, 2016.

[29]   R. G. Ross, "Interface design considerations for terrestrial solar cell modules," *Photovolt. Spec. Conf. 12th IEEE*, vol. 1, 1976.

[30]   I. Visoly-Fisher *et al.*, "Concentrated sunlight for accelerated stability testing of organic photovoltaic materials: Towards decoupling light intensity and temperature," *Sol. Energy Mater. Sol. Cells*, vol. 134, pp. 99–107, 2015.

[31]   E. Skoplaki, A. G. Boudouvis, and J. A. Palyvos, "A simple correlation for the operating temperature of photovoltaic modules of arbitrary mounting," *Sol. Energy Mater. Sol. Cells*, vol. 92, no. 11, pp. 1393–1402, Nov. 2008.

[32]   A. Larkin, J. D. Haigh, and S. Djavidnia, "The effect of solar UV irradiance variations on the earth's atmosphere," *Space Sci. Rev.*, vol. 94, no. 1–2, pp. 199–214, 2000.

[33]   L. Maturi, G. Belluardo, D. Moser, and M. Del Buono, "BiPV system performance and efficiency drops: Overview on PV module temperature conditions of different module types," *Energy Procedia*, vol. 48, pp. 1311–1319, 2014.

[34]   E. Skoplaki and J. A. Palyvos, "Operating temperature of photovoltaic modules: A survey of pertinent correlations," *Renew. Energy*, vol. 34, no. 1, pp. 23–29, Jan. 2009.

[35]   M. S. Buday, "Measuring irradiance , temperature and angle of incidence effects on photovoltaic modules in Auburn Hills , Michigan," 2011.

[36]   J. M. Chem, "Journal of Materials Chemistry," pp. 24265–24283, 2012.

[37]   N. Grossiord, J. M. Kroon, R. Andriessen, and P. W. M. Blom, "Degradation mechanisms in organic photovoltaic devices," *Org. Electron.*, vol. 13, no. 3, pp. 432–456, 2012.

[38]   A. K. Chauhan and P. Kumar, "Degradation in perovskite solar cells stored under different environmental conditions," *J. Phys. D. Appl. Phys.*, vol. 50, no. 32, p. 325105, 2017.

[39]   Z. Jiang *et al.*, "Amazing stable open-circuit voltage in perovskite solar cells using AgAl alloy electrode," *Sol. Energy Mater. Sol. Cells*, vol. 146, pp. 35–43, 2016.

[40]   S. M. S. and S. A. Melepurath Deepa, Manuel Salado, Laura Calio, Samrana Kazim, "Cesium

power: low Cs+ levels impart stability to perovskite solar cells," *Phys. Chem. Chem. Phys.*, no. 5, 2017.

Table 1 - performance parameters of MAPI and FMC modules on consecutive sunny days, comparing morning and afternoon characteristics measured at similar irradiances.

Module Type	Date	$T_{Ambient}$ (°C)	Irradiance (W/m²)	Time	I_{SC} (mA)	V_{OC} (V)	FF (%)	PCE (%)
FMC	17/06/17	20	276	08:15	12.63	3.70	35.84	4.66
				18:15	13.51	4.10	35.50	5.48
	18/06/17	23.4	293	08:15	12.62	3.60	33.99	4.05
				18:15	13.48	4.10	35.92	5.21
MAPI	17/06/17	19.1	283	08:15	8.09	4.00	31.55	2.77
				18:15	6.95	3.90	25.60	1.88
	18/06/17	19.6	296	08:15	7.94	3.90	32.06	2.57
				18:15	6.17	3.70	27.05	1.60
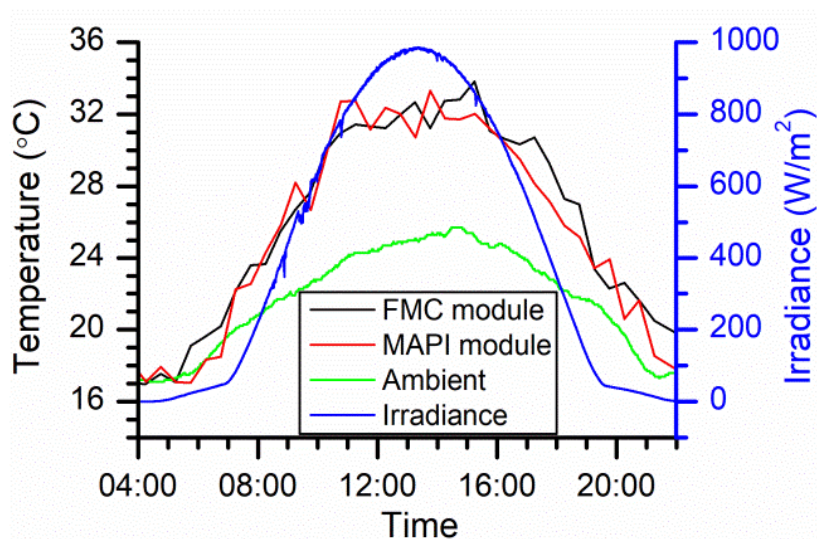
Figure 1: Irradiance (in-plane), ambient and module temperatures on selected sunny day (17/06.2017).
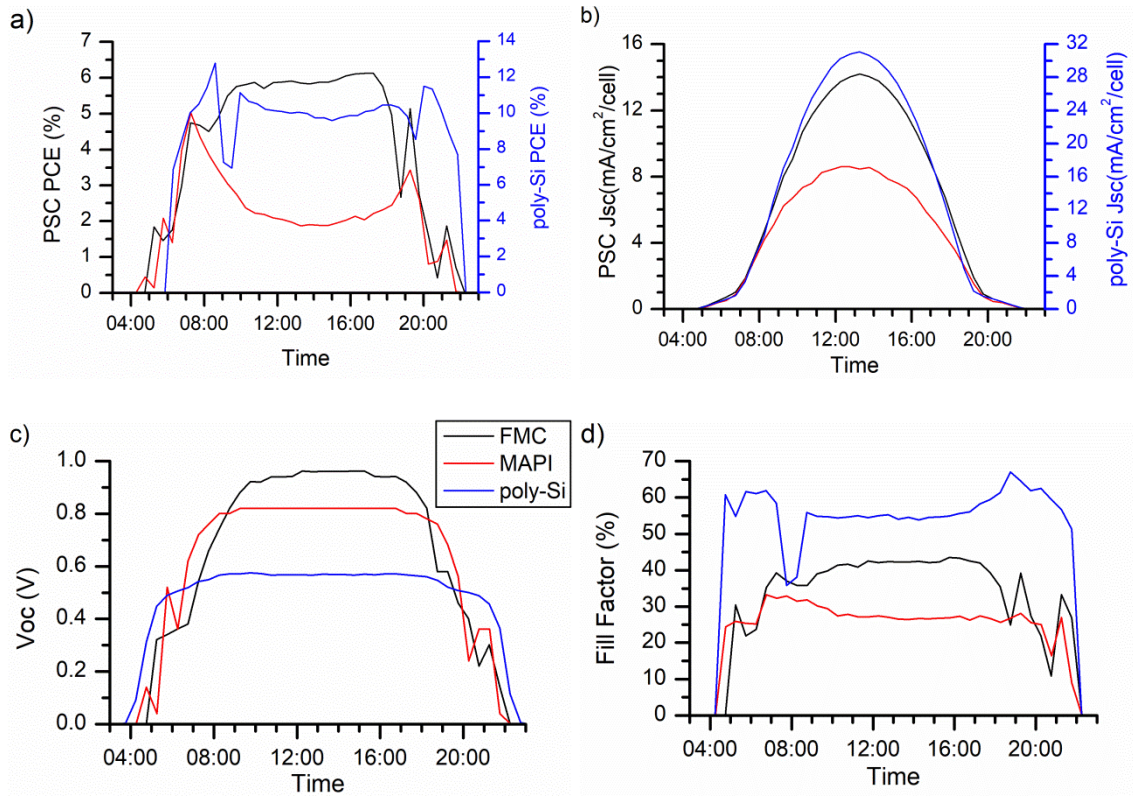
Figure 2 – Diurnal performance of PSC mini-modules on a sunny day in summer (17/06/2017) compared against diurnal performance of poly-Si module.
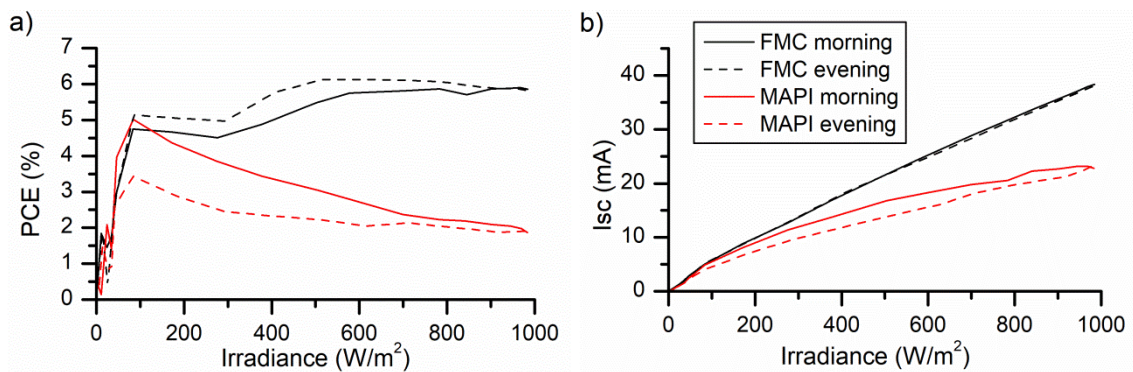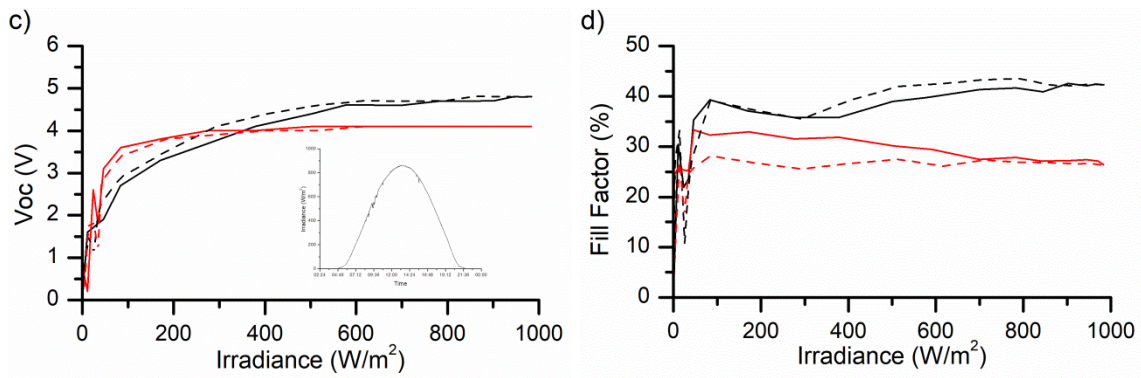
Figure 3: The PV performance parameters as a function of irradiance for PSC module shows the diurnal hysteresis of PSC mini-modules on a sunny day in the summer (17/06/2017): a) PCE, b) I$_{SC}$, c) V$_{OC}$ (inset shows the diurnal irradiance), and d) FF. The data also shows indirectly the temperature dependency as temperature varies as a function of incident irradiance.
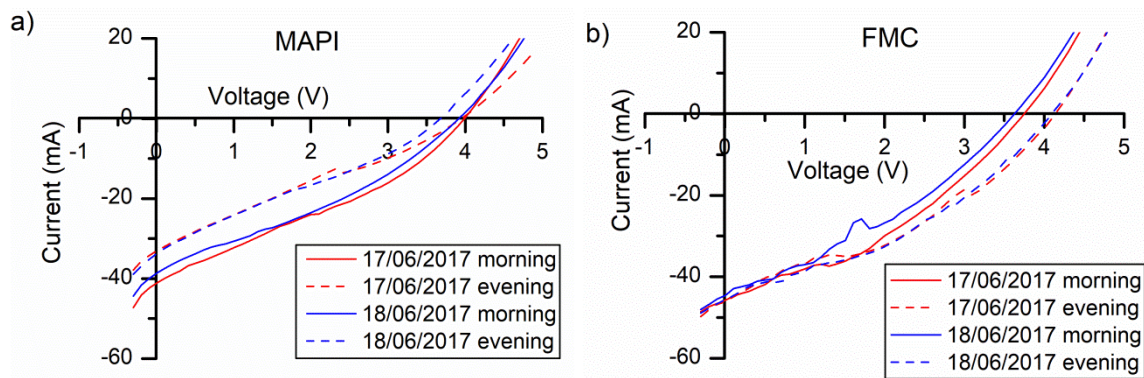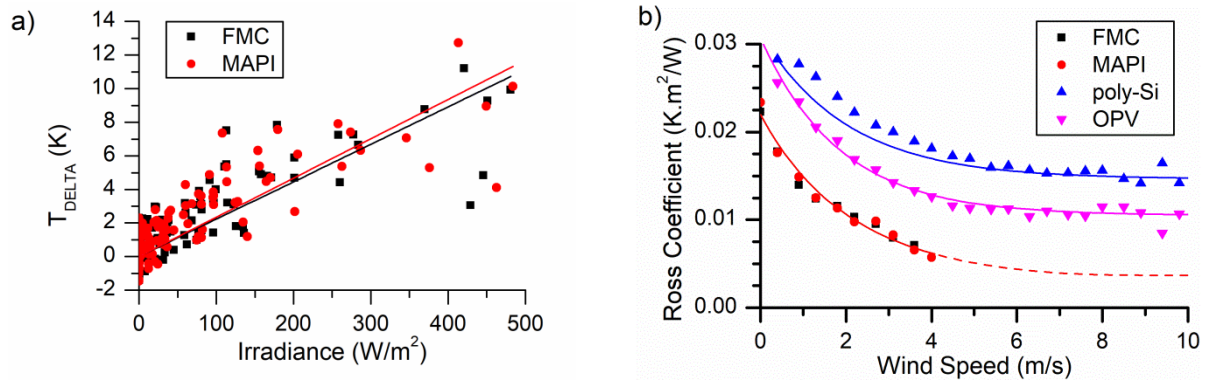

Figure 4 – Comparison of IV curves taken in the morning (solid) and afternoon (dashed) on two consecutive sunny days [current linearly adjusted to 1000 W/m²]: a) MAPI, and b) FMC.
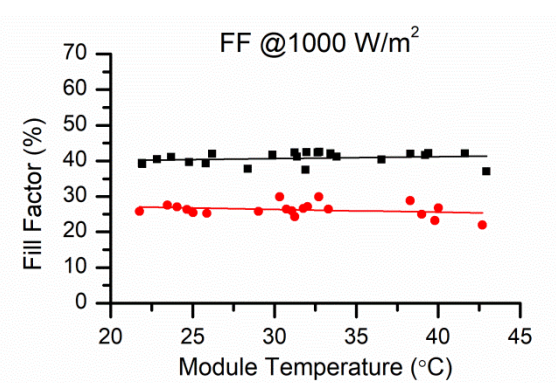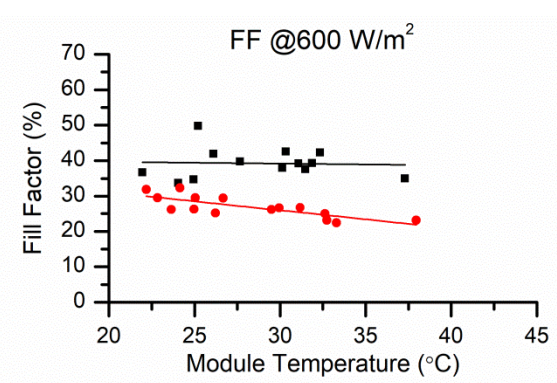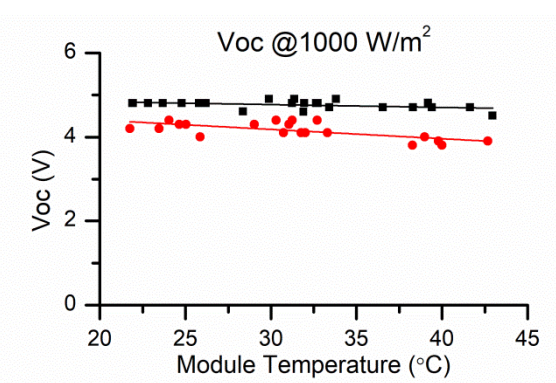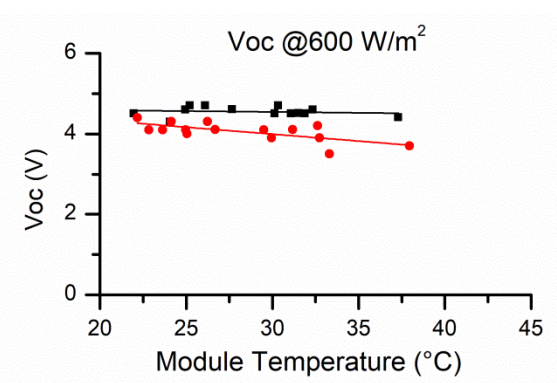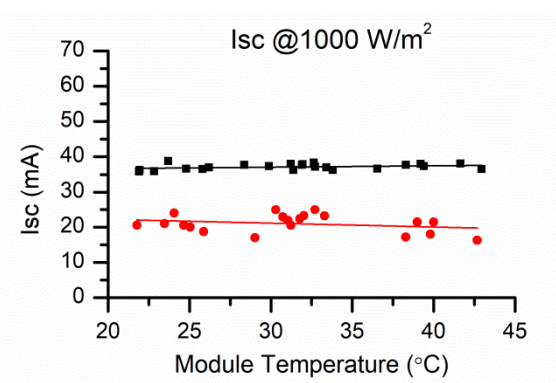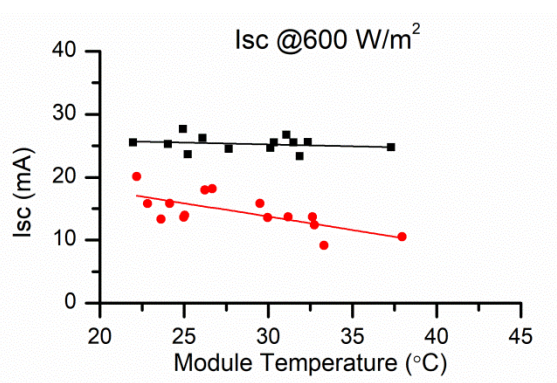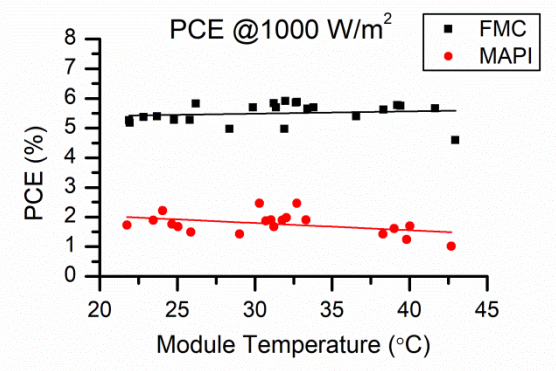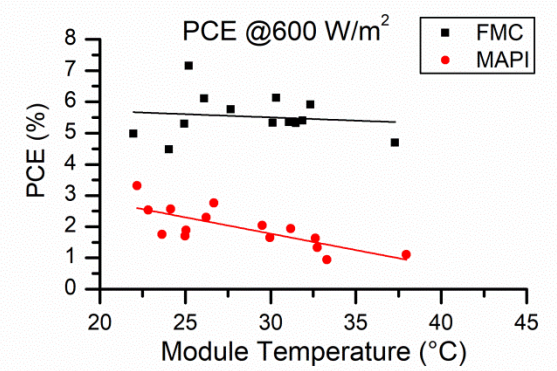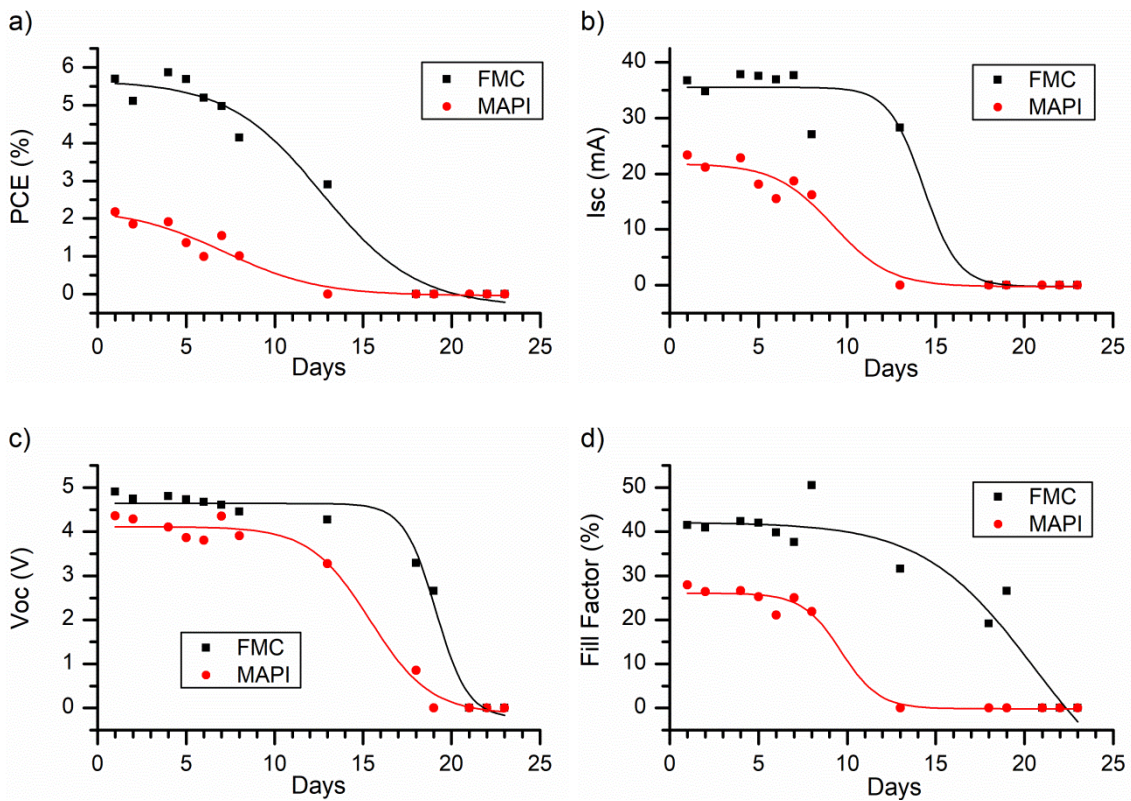
Figure 5 – Temperature dependence of PCE, I_{SC}, V_{OC} and FF measured at 600 W/m^2 and 1000 W/m^2. Fitter curves assisting in measuring the temperature coefficient

Figure 6: a) Module temperature above ambient vs. irradiance for the FMC and MAPI modules showing linear trend lines. b) Effect of wind speed on the Ross coefficient for various module types.

Figure 7 – Degradation in performance parameters measured at 600 W/m^2 in the summer of 2017.
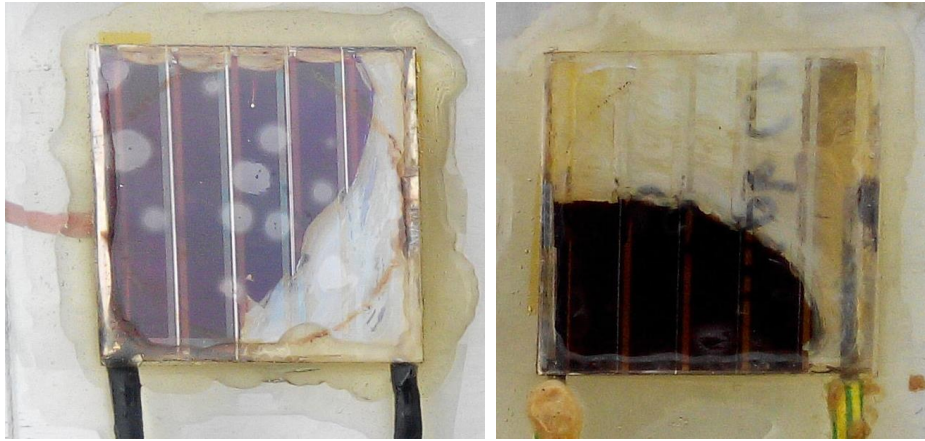
Figure 8 – Degraded PSC mini-modules after water ingress three weeks after outdoor installation.